Thick-GEM Based Trigger Detector Development for ALICE

Gergő Hamar and Dezső Varga

***Abstract*—Thick-GEM technology offers a robust and cheap outline which allows convenient simplifications of the detector design in comparison to MWPC-s.**

We show here the results from a prototype chamber, which was designed to test the operation principle of a future trigger detector for high p_T particles at the ALICE experiment at the CERN LHC. The basic idea is to detect the inclination of the tracks in the ALICE magnetic field; this way the smaller angle tracks, representing higher p_T, can be selected.

The prototype uses double layer TGEM with pad readout in Argon + CO_2, with different pad and TGEM layer geometries. Results from the data taking at the CERN PS beam facility are presented, demonstrating the applicability of the technology for high efficiency particle detection.

The achievable position resolution reduction at increased inclination angles is compatible with the widening of the charge deposit due to drift length. Sparking rate is found to be propotional to the particle rate, with relatively high frequency due to charge fluctuations of minimum ionizing particles. In conclusion, it is shown that such a system comprising four detection layers meets with the requirements of high p_T triggering at ALICE.

I. Motivation

A. VHMPID (Very High Momentum Particle Identification Detector)

Many theoretical models are trying to describe the nature of particle production in heavy ion collisions where the quarks and gluons may be forming the plasma (QGP). Interesting anomalies have been measured at RHIC in the 5 GeV/c $< p_T <$ 10 Gev/c region, especially at the unpredicted proton-pion ratios. This motivated Particle Identification (PID) to much higher momenta than originally planned at LHC ALICE.

Solving this problem Very High Momentum Particle Identification Detector (VHMPID) have been designed. VHMPID is a gas filled Ring Imaging Cherenkov detector which will be able to track-by-track distinguish pions, kaons and protons in the 5 GeV/c $< p_T <$ 25 Gev/c region.

Detector with this kind of PID will be useful for studying several physical question. Naturally one can look into deeper details of RHIC's proton pion ratio anomaly in a wider momentum region. In Pb+Pb collions one can study the effect of strongly intracting medium on the fragmentation functions. Moreover one can study the dihardon-/ multihadron-fragmentation functions via correlation of high momentum identified particles. Due to the special alignment of VHMPID it can bring a impove in jet analysis: near-side photon-hadron correlations will be measurable with the cooperation of the PHOS (PHOton Spectrometer), away side ones with the EMCAL (Electro-Magnetic CALorimeter). Furthermore high momentum charged particle identification allows the reconstruction of the still unknown high momentum region of the D, B mesons and Λ_c,Λ_b baryons.

VHMPID contains a 100 cm long box filled with CF_4 radiator gas. A spherical mirror at the end of the box reflects the emitted Cherenkov light, which forms a circle or ellipse shape at the front of the gas box. The photon sensitive chamber is separated with a CaF_2 window to maximize the quantum efficiency.

According to the ALICE trigger system and disc write capacity of ALICE and the low event rate at this high transverse momentum a factor of 40 can be saved in the recorded interesting data sample with a dedicated trigger.

B. HPTD (High P_T Trigger Detector)

The main idea of the triggering is to measure the inclination of tracks far from the interaction point (5 meters), tracks which are bent by the ALICE magnetic field (0.5 T). High momentum means small bending — or smaller inclination. The High P_T Trigger Detector (HPTD) contains 4 layers of TGEM based gaseous detectors, with fair spacial resolution in the direction of the azimuthal direction and reduced resolution in the direction of the field. Such a trigger detector needs high granularity (pads $< 2\ cm^2$) and high multitrack resolution.

The HPTD's gaseous detectors will not need to measure precise energy loss of the traversing particles, since their main purpose is to give information on the presence / non presence of the particle. Furthermore, with one bit output per channel the electronics may be cheap, simple and fast. In the final outline, the output bits will be combined in an FPGA logic to provide the necessary trigger signal to the ALICE L1 trigger system.

II. Setup

A. Thick-GEM

GEM (Gas Electron Multiplier) [1] technology has proven its reliability for experimental circumstances where good position resolution is to be combined with flexible detector construction. The Thick-GEM (TGEM) [2] on the other hand relaxes the demands on position resolution, but offers a robust and cheap outline which allows convenient simplifications of the detector design in comparison to MWPC-s.

Manuscript received November 14, 2008. This work has been supported in part by the Hungarian OTKA grants No. NK062044, IN71374, H07-C 74164.

G. Hamar is with the MTA KFKI RMKI Research Institute for Particle and Nuclear Physics, Budapest, 1121 Hungary (e-mail: hamargergo@rmki.kfki.hu).

D. Varga is with the Department of Physics, Eötvös University, Budapest, 1117 Hungary (e-mail: Dezso.Varga@cern.ch).

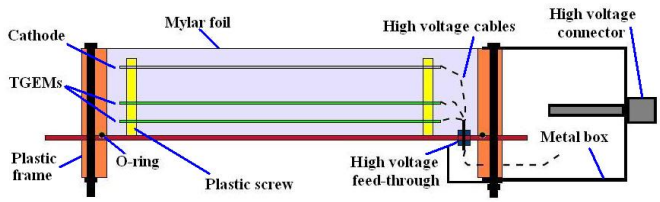

Fig. 1. Outline of the test chamber, seen from the side.

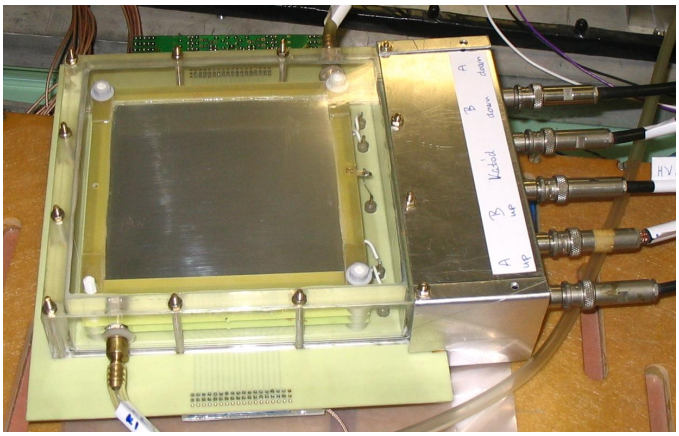

Fig. 2. Test chamber in the lab with each electrodes on different high voltage connections (in the beam tests, a single HV with resistor chain was used)

B. Chamber

Small and flexible test chambers have been built with 10x10 cm^2 active area (see Figure 1. and 2.). In the chambers, the drift, transfer and induction gaps, as well as the number of TGEM layers were simple to vary during the first optimization process. For the actual data taking at the CERN PS test beam, we used double Thick-GEMs with thickness 400 μmm, hole diameter 300 μm, 600 μm pitch. Cathode and TGEM voltages were set by a resistor chain, with voltage ratios of 20:30:20:30:40 for the drift, first TGEM, transfer, second TGEM, and induction fields, respectively. Both the transfer and induction gaps were 3 mm wide. For the pad readout we used 5 mm $\times$ 50 mm (and in the second chamber 2.5 mm $\times$ 50 mm) size pads according to the requirements of the HPTD.

C. Beam Setup

The results presented in this paper are based on a data taking at the CERN PS facility. The beam was around 6 GeV positive particles (mostly pions). The coincidence of a pair of scintillators (before and after the chambers) were used to trigger the beam particles.

D. Electronics

In the test chambers, for each pads an analog preamplifier stage was followed by a discriminator with variable threshold. For a number of studies the analog output of the preamp stage was directly read out and studied either on a storage scope or digitized on a multi-channel ADC. The pads on each channel presented a typical of 20 pF input capacitance, and charge collection time for the 1 cm gap required 600 ns integration time. The total noise was found to be below 10^4 electrons per channel.

For the final design, the discriminated (one-bit digitized) signal is to be stored in a shift register, and read out in a multiplexed mode with frequencies up to 40MHz. Such prototype electronics was also used in the test beam data taking, where each card handles 16 channels, and 4 cards (64 channels) were read out in a daisy chain into a PC.

III. Results

A. Analog signal shape

The analog signal starts with a negative pulse, followed by a positive overshoot to compensate the zero output charge. The typical signals are shown in Figure 3. The reason for such a strong clipping (large overshoot) was to reduce the total signal

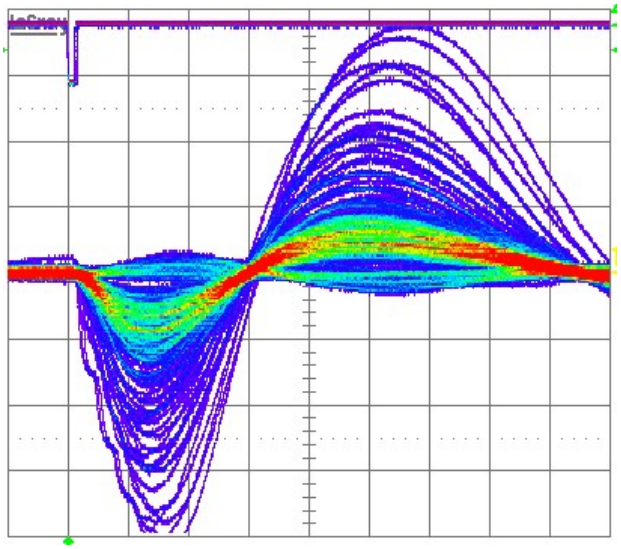

Fig. 3. Analog output signals on the storage scope screen. Noise and signal are well visible, as well as the negative signal / overshoot structure.

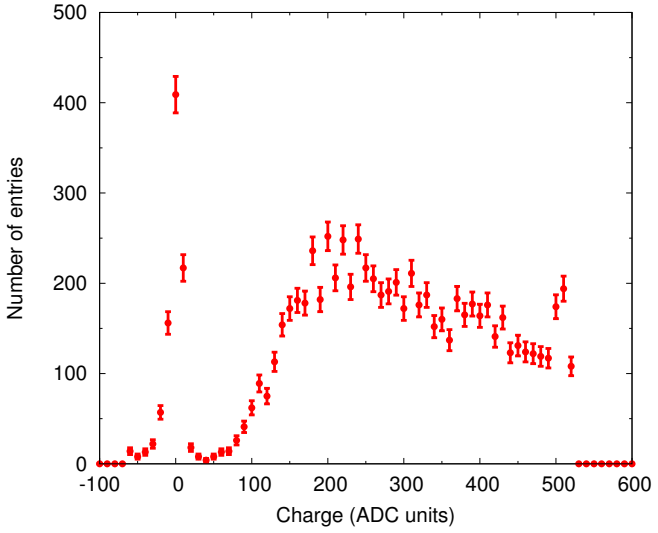

Fig. 4. Measured charge distribution for the central pad with focused beam. The saturation is due to limited dynamic range.

length, in accordance with the LHC heavy ion beam bunch crossing.

The analog signals were measured with Camac ADC-s, using 200 ns gate width centered on the negative peak, at a delay of about 400 ns. Figure 4. shows the charge distribution of the pad where the beam was approximately centered. The Gaussian-shaped noise and the Landau-shape signal are well separable. At high charges, the electronics saturation casues distortion: the dynamic range is on purpose chosen to be limited, to allow for a simpler adjustment of the discrimination level.

B. Correlations, cross-talk

In Figure 5 the two different type of cross-talk effects are distinguishable. If the electron cloud of the gas multiplication process spreads over more than one pads, the correlation is positive; evidently higher charge deposit corresponds to stronger cross-talk. Futher cross-talk effects are caused by capacitive coupling between neighbouring pads, and between the TGEM lower electrode and the pads. This latter causes a change of the signal (opposite to the normal pulse) on all pads; such effects may be reduced later by introducing a capacitor between TGEM lower electrode and the ground. To quantify the cross-talk effects, the beam was focused on one specific pad in the middle region of the chamber. The signal on the neighbouring pads were measured as a function of the charge on the central pad. In Figure 6 the signal on the neighbouring pad was separated into two classes: either below noise threshold (around 50 counts on Figure 4) or above. It is interesting to note that the mean signal in the two classes behave differently: the signals below noise level show negative correlation (capacitive coupling) whereas the signals above nosie level indicate positive correlation (spread of charge). The large errorbars of the latter are due to the fluctuations in the Landau-tail of the total charge deposit.

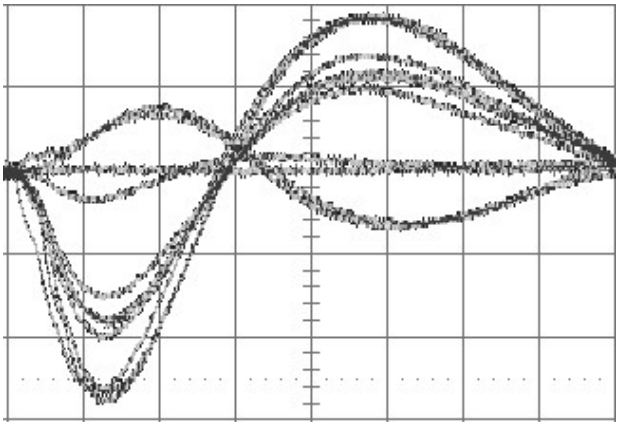

Fig. 5. Signals on neighbour of central pad: besides ”normal” signals, negative correlated signals are visible (see text for discussion)

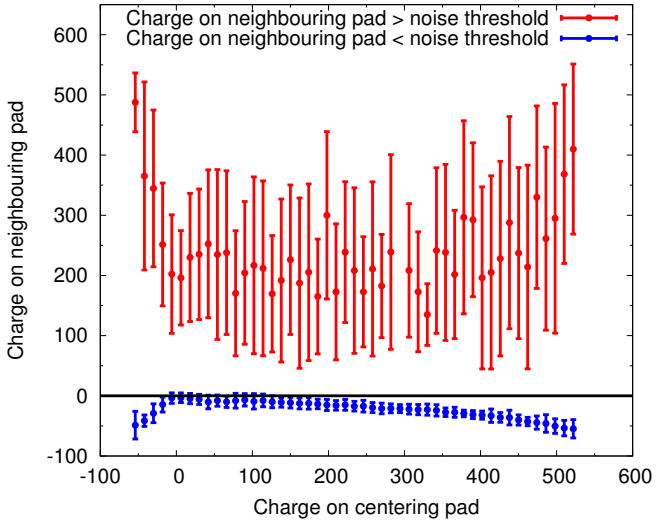

Fig. 6. Approximate size of correlation (cross talk) on the neighbour of central pad (on which the beam is focused). Capacitive cross-talk causes negative correlation (blue symbols), charge spread and pad-by-pad cross-talk causes positive correlation.

C. Eficiency

The measurements below are aimed at assessing the performance of the discriminated (1 bit digitized) multiplexed prototype readout. The most straight-forward quantity to measure was the counting efficiency as a function of the applied high voltage on the TGEM-s, as a function of the discrimination level, and using different gas mixtures. The discrimination level is a relative quantity, the ”zero” signal corresponds approximately to 2.1V, and the noise RMS is about 0.2V.

The efficiency as a function of the TGEM high voltage is shown in Figure 7. and Figure 8., at different discrimination levels and using different Ar+CO_2 gas mixtures. It is to be noted, as clearly visible on Figure 8, that the efficiency decreases slowly after a maximum, which is due to empty events after sparking: such effects are discussed in Secion ”Sparks”.

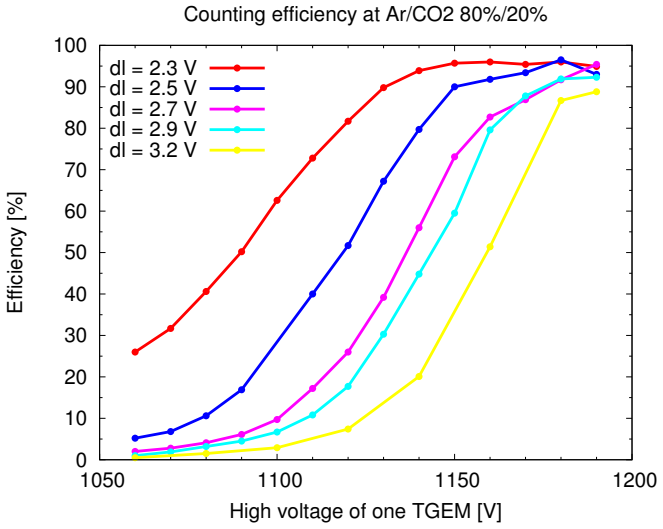

Fig. 7. Counting efficiency of the chamber versus the applied TGEM's voltage at different dicrimination levels. The meaning of the effective discrimination level (dl) is discussed in the text.

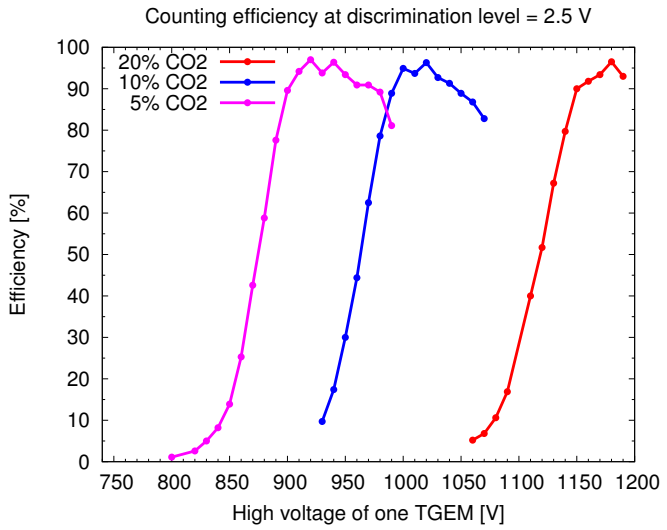

Fig. 8. Efficiency curves for different gas mixtures. The efficiency drop caused by increased sparking rate is apparent for all cases

D. Angular smearing

The support frame of the chamber was rotatable from 0 to 60 degrees inclination (0 means perpendicular beam on the chamber surface). For the HPTD purpuses, the study of angular effects is necessary, since most tracks will enter at large inclination. Assuming small widening of the deposited charge due to the inclined tracks entering at angle α, the increase of the number of pads in one hit is expected to be the following:

$$\langle n \rangle_\alpha^2 = \langle n \rangle_0^2 + (2 \cdot tan(\alpha))^2$$

if maximum efficiency is reached for all angles. At large angles however, the particle distributes the charge over many pads, and if its path reduces, the detection efficiency drops. In Figure 9., the average number of pads per hit is shown as a function of the inclination angle, demonstrating on one hand the applicability of the above formula up to about 30 degrees, and on the other hand the reduction of the effective "smearing" at higher angles.

E. Sparking

In order to safely detect sparks off-line, we have developed a straightforward and reliable method, which exploits the fact that the efficiency of the chamber drops to zero after the spark. This "blinding" of the chamber will appear as long sequence of events without chamber hits. In Figure 10. the length distribution of empty event sequences is plotted, clearly demonstrating that sparks are creating statistically very relevant pattern.

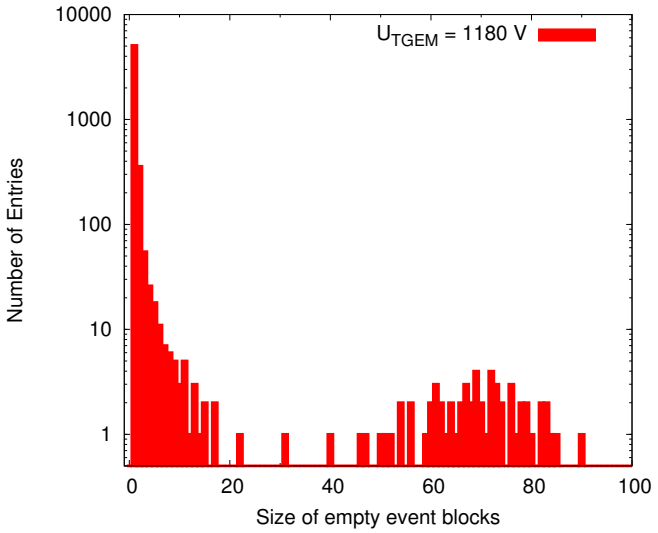

Fig. 10. Distribution of empty event sequence length. The sparks are well separated, appearing as long (typically 60-80 events for this specific setup) "empty train".

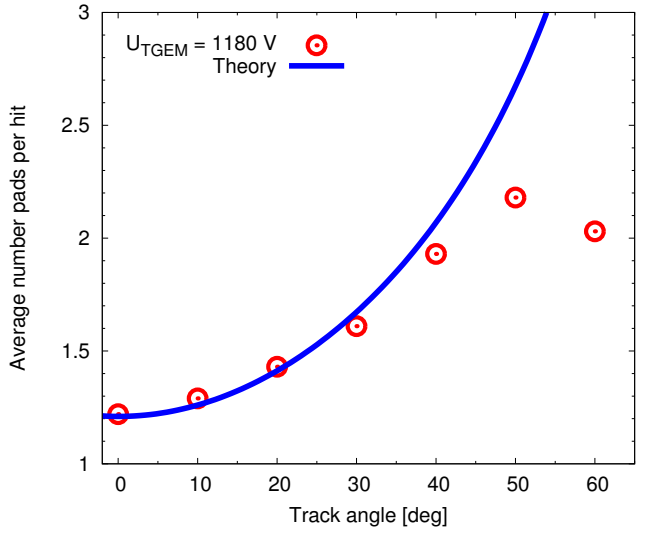

Fig. 9. Angular smearing: the increase of average number of firig pads per hit compared to a simple square-sum rule (see text for discussion).

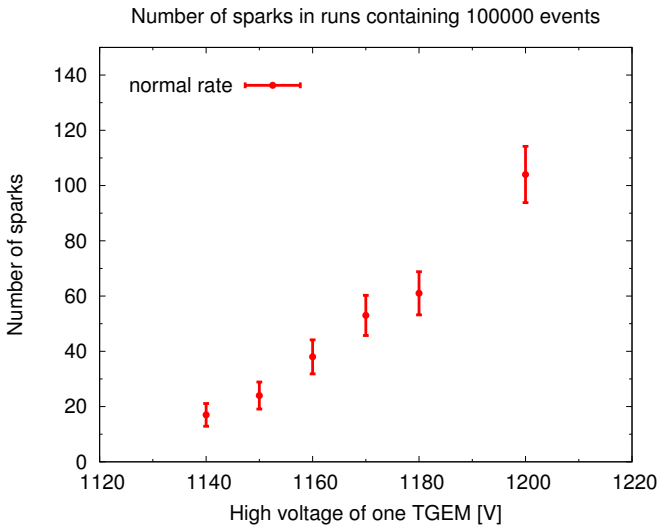

Fig. 11. Spark number (for 100k events) as a function of the TGEM high voltage.

Our studies have shown that the pobability of sparking at a given beam rate increases with the TGEM high voltage, see Figure 11. However, the function is not directly proportional to the multiplication gain, which is to be confirmed and understood by further studies.

The sparking probability on the other hand is proportional to the beam rate; from Figure 12. it is clear that the sparking probability per event reaches a per-mille level already at beam rates in the order of $10kHz/cm^2$, which is a rather low figure in comparison to the usual "high beam rate" studes. The reason is probably connected to the high ionizing Landau-tail of the minimum ionizing particles; and also points on the fact that such spark studies need indeed to use particles instead of gamma rays or UV light (single photo-electrons).

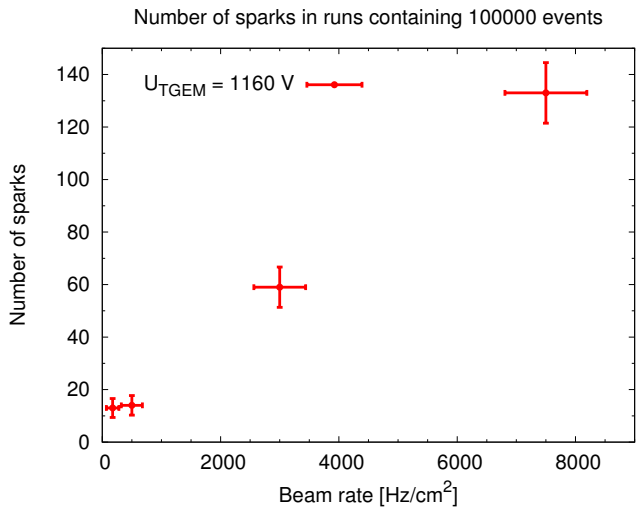

Fig. 12. Spark number (for 100k events) as a function of beam rate. The proportional behaviour is clearly visible.

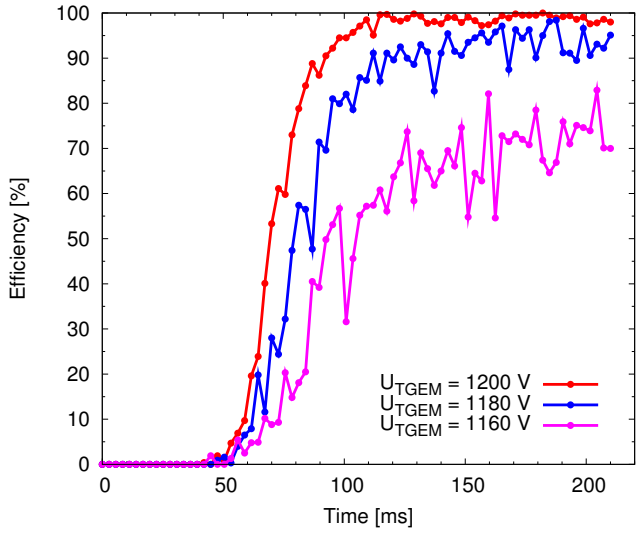

Fig. 13. Recovery of the chamber after sparks: Efficiency as a function of time after the appearance of a spark (beginning of a long empty event train)

The sparking shuts down the chamber for about 50 ms in our specific setup. After that the chamber recovers slowly, and reaches full gain after 100 ms. This recovery time corresponds reasonably to the expected time constant of the chamber, with resistors in the 10 Mohm and TGEM capacity in the 1 nF range. The recovery curve is shown in Figure 13.

IV. Conclusion

The physics motivation of the VHMPID system is particle identification at high (transverse) momentum at the CERN ALICE experiment. Such measurements are expected to largely improve by a trigger system. Our studies have confirmed the applicability of TGEM technology as a very promising choice for this task. The achievable efficiency already with the preliminary test system is above 98%, whereas the position resolution including angular smearing behaves as expected. Sparking presents a specific challenge for TGEM technology, which we have analyzed on the data set off-line. We have concluded that sparking remains controllable at beam rates expected at the CERN ALICE experiment (in the order of $100Hz/cm^2$) whereas at beam rates two orders of magnitude larger than this, sparking raises a serious concern (reaching probability of 10^{-3} per track).

Acknowledgment

This work has been supported in part by the Hungarian OTKA grants No. NK062044, IN71374, H07-C 74164.

References

[1] F.Sauli (1997) Nucl.Instr.and Meth. **A386** 531
[2] R.Chechik, A. Breskin, C. Shalem (2005) Nucl.Instr.and Meth. **A553** 35